Temperature Effects and Temperature-Dependent Constitutive Model of Magnetorheological Fluids

Haopeng Li[1,2], Ilari Jönkkäri[2], Essi Sarlin[2] and Fei Chen[1*]

[1] School of Mechatronic Engineering, China University of Mining and Technology, No.1, Daxue Road, Tongshan Zone, Xuzhou, Jiangsu Province 221116, China

[2] Faculty of Engineering and Natural Sciences, Tampere University, Korkeakoulunkatu 6, 33720 Tampere, Finland

[*] cfcumtxz@126.com

Rheol Acta (2021). https://doi.org/10.1007/s00397-021-01302-3

Abstract: The knowledge of the temperature effect on magnetorheological fluid is critical to accurate control of magnetorheological devices, since the temperature rise during operation is unavoidable due to coil energization, wall slip, and inter-particle friction. Based on a typical commercial magnetorheological fluid, this work investigates the effect of temperature on magnetorheological properties and its mechanisms. It is found that temperature has a significant effect on the zero-field viscosity and shear stress of magnetorheological fluid. The Herschel-Bulkley model that has high accuracy at room temperature, does not describe accurately the shear stress of magnetorheological fluids at high temperatures, as its relative error is even up to 21% at 70 °C. By analyzing the sources of shear stress in magnetorheological fluids, a novel constitutive model with temperature prediction is proposed by combining the Navier-Stokes equation and viscosity-temperature equation. The experimental results show that the error of the novel constitutive model decrease by 90% at different temperatures and magnetic field strengths, exhibiting an excellent accuracy. This temperature-dependent constitutive model allows the properties of an MR fluid to be widely characterized only in a few experiments.

Keywords: Magnetorheological fluid, Shear stress, Temperature effect, Constitutive model

1. Introduction

Magnetorheological (MR) fluid is a smart material consisting of soft magnetic particles, base carrier fluid, and surfactant additives. MR fluid appears as a liquid-like state in the absence of a magnetic field, while it instantly changes into semi-solid state with a controlled yield stress when a magnetic field is applied. This state transformation is reversible. Because of the controllable MR characteristics, MR fluids have been widely used in power transmission (Kikuchi et al. 2020), vibration control (Yoon et al. 2021), sealing (Kubik et al. 2019), finishing (Arora and Singh 2020), and other fields.

In MR devices, especially in MR transmission devices, heat is generated resulting in temperature rise, due to the coil energization (Chen et al. 2015), inter-particle friction, and wall slip (Chen and Yang 2019). With an increase in shear rates, the heat generation will be further intensified, which will harm the performance of MR fluids (Sahin et al. 2009). This has aroused the interest in studying the thermal conductivity of MR fluids (Maroofi and Hashemabadi 2019, Yildirim and Genc 2013) and the preparation of MR fluids with high-temperature resistance (Tian et al. 2019), but the optimized design of MR devices for better heat dissipation is the most common way to deal with the temperature rises. Even so, the unavoidable temperature rises will cause errors in the MR models, and also affect the control accuracy of MR devices.

In previous studies, the effect of temperature rise on MR properties has been mainly attributed to the effect on shear yield stress. The research results of Sahin *et al.* (Sahin et al. 2009), Yahya *et al.* (Rabbani et al. 2015) and Bahiuddin *et al.* (Bahiuddin et al. 2018) have shown that the shear yield stress decreases with increasing temperature. Wu *et al.* (Wu et al. 2016) have demonstrated that the effect of temperature on yield stress is mainly due to the decrease in saturation magnetization strength, but it occurs at ultra-high temperatures more than 200 °C, which has also been proven by Wang *et al.* (Wang et al. 2014). MR devices, especially high-power devices, are designed to avoid ultra-high temperatures through heat dissipation channels. Besides, the operating temperature of MR fluids is usually less than 100 °C, and the maximum operating temperature does not exceed 150 °C for most MR fluids.

The previous studies have explored the temperature effect on the properties of MR fluids, but its mechanisms are still to be revealed. Besides, a precise model needs to be established to predict the temperature-dependent properties of MR fluids. In this paper, a typical commercial MR fluid is investigated to reveal the effect of temperature rise on the MR properties, as well as its mechanisms. On this basis, a novel temperature-dependent constitutive model is proposed and verified. This paper succeeds in revealing the mechanisms of temperature on the properties of the MR fluid and allows the properties of an MR fluid to be widely characterized only in a few experiments.

2. Constitutive Models of MR Fluids

A model that can describe the shear stress of MR fluids accurately is important for the preparation of MR fluids, as well as the design of MR devices. In this regard, scholars are committed to find a suitable model to describe the properties of MR fluids. Several models, such as the Biviscous model (Williams et al. 1993), the Eyring model (Choi et al. 2005), the Papanastasiou model (Papanastasiou 1987), the Mizrahi–Berk model (Pelegrine et al. 2002), the Robertson-Stiff model (Cvek et al. 2016) and the Rosensweig model (Rosensweig 1995) have been proposed, but the Bingham model (Saha et al. 2019), the Casson model (Malik et al. 2016) and the Herschel-Bulkley model(Desai et al. 2020) are most commonly used, which are originally employed to describe the properties of non-Newtonian fluids that have a yield stress. The Bingham model evolves from the Newtonian fluid model and its constitutive equation is

$$\tau = \tau_0 + \eta_0 \dot{\gamma} \quad (\tau \geq \tau_0) \quad (1)$$

where τ_0 is the shear yield stress of the MR fluid under the applied magnetic field, η_0 is the dynamic viscosity, and $\dot{\gamma}$ is the shear rate. The Bingham model assumes that the shear stress of MR fluids increases linearly with the shear rate after yielding, where the viscosity remains constant like Newtonian fluids. Different from the Bingham model, the Casson model highlights shear thinning by adding the small behavior index ½, of which the constitutive equation is

$$\tau^{\frac{1}{2}} = \tau_0^{\frac{1}{2}} + \eta_\infty^{\frac{1}{2}} \dot{\gamma}^{\frac{1}{2}} \quad (\tau \geq \tau_0) \quad (2)$$

where η_∞ is the Casson viscosity that is usually obtained at high shear rates. The Casson model can well describe the MR behavior in the post-yield region, but it ignores the shear thinning effect in the pre-yield region. Besides, the Casson model is not sensitive to the rheological behaviors of the MR fluids (Lv et al. 2018). The Herschel-Bulkley model is derived from the power-law fluid model, and its constitutive equation is

$$\tau = \tau_0 + k\dot{\gamma}^n \quad (\tau \geq \tau_0) \quad (3)$$

where k is the flow consistency coefficient and n is the flow behavior index. The fluid is Newtonian if n=1, shear thinning if n<1 and shear thickening if n>1. The Herschel-Bulkley model will become the Bingham model when the viscosity of a fluid is constant, but for MR fluids, n is usually less than 1, meaning that MR fluids will become thinner as shear rates rise. The Herschel-Bulkley model is a three-parameter constitutive model, so that it can well describe the MR effects in both pre-yield and post-yield regions by the variable parameters.

Based on a homemade MR fluid, Lv *et al.* (Lv et al. 2018) made a comparative experimental study on the above three models, in which the comparison and application scope are well summarized. The following conclusions were obtained:

a) All three models can well describe the properties of MR fluids in the absence of a magnetic field.

b) The Casson model can only be used to describe the mechanical behavior of MR fluids with a lower yield stress after complete yielding.

c) Herschel-Bulkley model can predict the shear stress of the MR fluid nonlinearly changing with an applied magnetic field.

However, the above constitutive models are established at room temperature, while the effect of temperature rise on the constitutive model need to be explored. In the condition of temperature rise, whether the constitutive model can be still used is also to be investigated, which is of great significance to describe the MR effects accurately.

3. Materials and measurements

3.1 Materials

A typical commercial MR fluid MRF 132DG (LORD) was used in this research, of which the parameters are shown in Table 1.

Table 1 Parameter of MRF 132DG (LORD)

Mass fraction	Density	Viscosity @ 40 ℃	Operating temperature
80.98 wt%	2.95-3.15 g/cm^3	0.112 ± 0.02 Pa·s	-40 ℃ to +130 ℃

To separate the base carrier fluid for analysis since its formulation is not public, the MRF 132DG was placed in a test tube for 60 days. The MRF 132DG showed significant sedimentation with a clear brownish-red liquid precipitated from it. This liquid should contain the base carrier fluid, as well as the surfactants dissolved into the base carrier fluid. The dose of surfactants is usually quite low, so the effect of the dissolved surfactants on the base carrier fluid properties can be considered minor.

3.2 Measurements of MR effects

Anton Paar MCR 301 rotational rheometer was used to measure the rheological properties of the MR fluids. The measurements were carried out with and without an applied magnetic field. In the absence of a magnetic field, a concentric cylinder module was applied because this module with a large shear surface shows excellent sensitivity, especially when the liquid has low viscosity. Besides, the module can effectively reduce the error caused by the centrifugal force during rotation. The concentric cylinder module is composed of a rotating inner cylinder and a stationary outer cylinder where there is an annular gap of 0.71 mm to hold the MR fluid, as shown in Figure 1. The rotating cylinder is made of stainless steel with a rough surface to avoid slip, while the stationary cylinder is made of aluminum. The apparent viscosity of the MR fluid was measured at the shear rates from 0.01 s^{-1} to 100 s^{-1}.

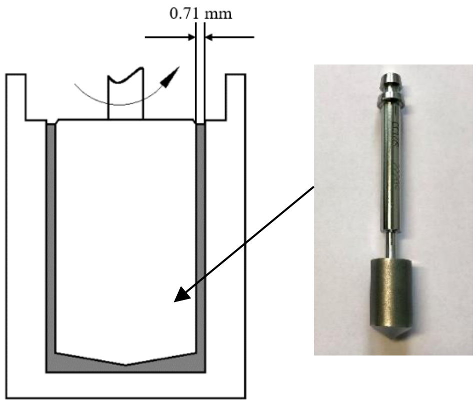

Figure 1 Scheme of concentric cylinder module for MCR 301

The rheometer was equipped with an MRD 180/1T MR module to measure the properties of MR fluids under magnetic fields, as illustrated in Figure 2. The MR module is composed of a rotational top plate and a fixed bottom plate where there is a 1 mm gap between the top and bottom plates to hold MR fluids. The MR module also contains an exciting coil that generates a vertical magnetic field through the current control module. The magnetic field passes vertically through the testing gap by upper and lower yokes, as shown by the red arrows in Figure 2. The contact surfaces of both top and bottom plates are made of aluminum with grooves to reduce the errors from wall slip, which is described in detail in a previous work (Jonkkari et al. 2013). The exciting current was set to achieve a suitable magnetic field strength for each measurement according to Figure 3. The test temperature (from 20 ℃ to 70 ℃) was controlled by water circulation. The apparent viscosity and shear stress of the MR fluid were obtained while increasing the shear rate logarithmically from 0.01 s^{-1} to 100 s^{-1}.

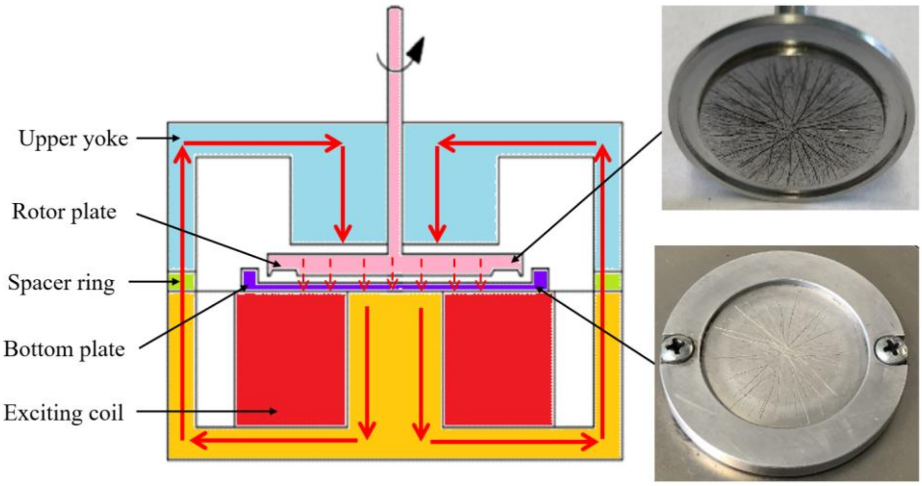

Figure 2 Scheme of MRD180/1T MR module for MCR 301

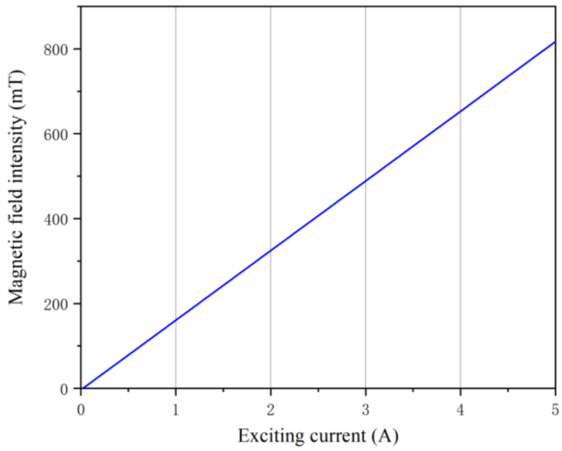

Figure 3 Magnetic field strength of shear gar under different exciting current

4. Temperature effects

4.1 Zero-field viscosity

Apparent viscosity and shear stress are the most important indicators of the MR effect, and they vary with the same law according to the operating principle of the rheometer. In the absence of a magnetic field, the apparent viscosity of the MR fluid was obtained experimentally at different temperatures, as shown in Figure 4.

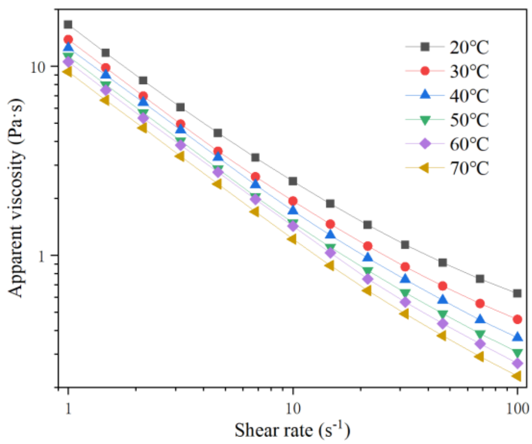

Figure 4 Zero-field viscosities of MRF 132DG at different temperatures

As can be seen from Figure 4, the viscosity of MRF 132DG gradually decreases with the increase of shear rates, indicating that the MR fluid is a non-Newtonian fluid even in the absence of a magnetic field. The increase in temperature leads to lower zero-field viscosity of the MR fluid. At higher shear rates, the difference in zero-field viscosities of an MR fluid gradually widens at different temperatures. For example, at steady-state shear (100 s^{-1}) the zero-field viscosity decreases by 51.0% when the temperature rises from 20 ℃ to 50 ℃ and it decreases by another 12.4% when the temperature increases to 70 ℃.

4.2 Shear stress

Under the magnetic field of 325 mT, the shear stress of MRF 132DG was measured at different temperatures, as shown in Figure 5.

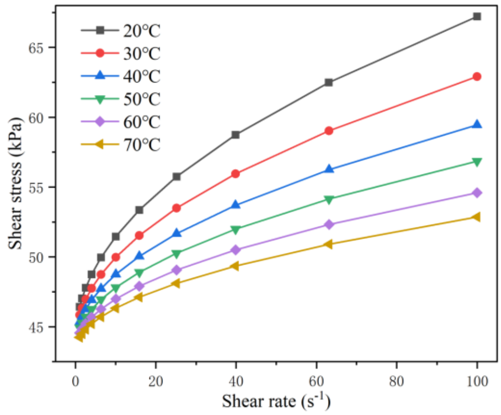

Figure 5 Shear stress of MRF 132DG at different temperatures

It can be seen from Figure 5 that the shear stress of MRF 132DG increase with the shear rate, but its increase rate slows down, presenting the obvious property of non-Newtonian fluid. At the same shear rate, the shear stress decrease with temperature rises. When the shear rate increases, the decrease of shear stress caused by temperature rising becomes more obvious. For example, at the shear rate of 10 s^{-1}, the shear stress decreases from 51.47 kPa to 47.82 kPa, decreasing by 7.1% when the temperature rises from 20 ℃ to 50 ℃. However, at the shear rate of 100 s^{-1}, the shear stress decreases from 67.22 kPa to 56.85 kPa, decreasing by 15.4%. It is not difficult to predict that the shear stress loss caused by temperature rise will become more significant as the shear rate continues to increase.

It is well known that one of salient properties of MR fluids is the field-dependent shear stress with respect to the shear rate. Therefore, the temperature effect on the properties of MR fluids was also analyzed by applying different magnetic fields, as shown in Figure 6.

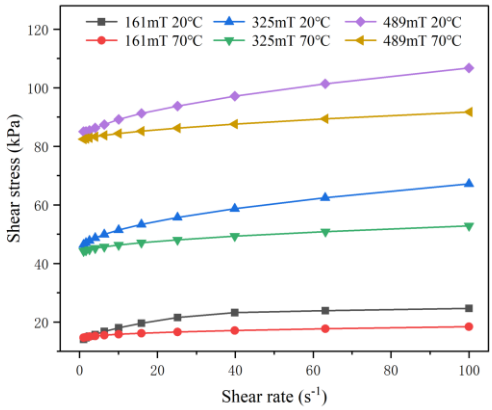

Figure 6 Shear stress of MRF 132DG under different magnetic field strengths and temperatures

It can be seen from Figure 6, as the magnetic field strength increases, the shear stress of MRF 132DG increases at the same shear rate, which is due to the increased magnetic force between particles. At the same shear rate, the temperature has a more obvious influence on the shear stress as the magnetic field strength increases. When the temperature rises from 20 °C to 70 °C at the shear rate of 100 s^{-1}, the shear stress decreased by 6.24 kPa, 14.35 kPa and 15.03 kPa under the magnetic field of 161 mT, 325 mT and 489 mT, respectively. However, the influence degree of temperature rise on shear stress gradually decreases, of which the percentage is 25.3%, 21.4%, and 14.1% for the same working conditions mentioned above, respectively.

4.3 Constitutive models

It has been proven that the Herschel-Bulkley model has the best fit for the commercial MR fluid with high mass fractions (Lv et al. 2018). At room temperature (20 °C), the shear stresses were obtained at 325 mT and the Herschel-Bulkley model was used to fit the experimental data. Then the temperature was set to 70 °C and the shear stress was obtained again at the same magnetic field, as shown in Figure 7.

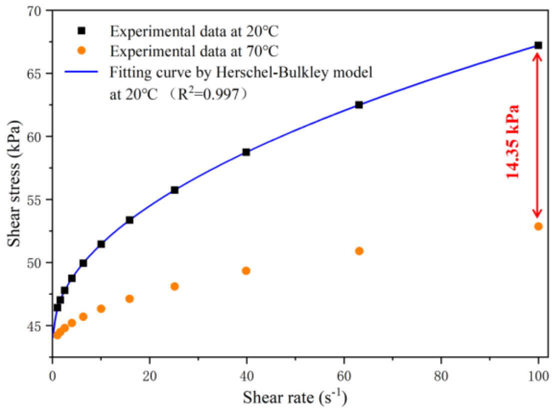

Figure 7 Shear stress and Herschel-Bulkley model at 20 °C and shear stress at 70 °C for MRF 132DG

As can be seen from Figure 7, the Herschel-Bulkley model is no longer able to accurately describe the shear stress of the MR fluid at 70 °C. Its error is 10.0% at 10 s^{-1} while it reaches up to 21.4% at 100 s^{-1}. It can be expected that the error of the Herschel-Bulkley model will continue to increase with temperature rising. As a consequence, a temperature-dependent constitutive model should be proposed to predict the MR effects at different temperatures.

It should be noted that, although the shear stress has a significant decrease with temperature, the yield stress barely changes, with the values of 44062 Pa and 43267 Pa at 20 °C and 70 °C, respectively, decreasing only by 1.8%.

5. Discussion

5.1 Temperature-dependent constitutive model

The constitutive models divide the shear stress into magnetic stress and non-magnetic stress where the non-magnetic stress includes the forces within base carrier fluid, as well as between particles and base carrier fluid. The shear stress is the sum of the forces by which the MR fluid resists shear, and it can be divided into three parts according to the source as shown in Equation (4):

$$\tau = \tau_m + \tau_\eta + \tau_h \quad (4)$$

where τ_m is the sum of the force between particles, τ_η is the sum of the force in base carrier fluid, and τ_h is the sum of the force between particles and base carrier fluid.

(a) Force between particles τ_m

As mentioned in the Introduction, the material with good thermal stability is usually selected as the soft magnetic particles. Previous studies (Wu et al. 2016, Wang et al. 2014) have found that the temperature rise will not cause the decrease in the saturation magnetization when the temperature is below 200 °C. Further, in section 4.3, it is proved that the shear yield stress barely decreases, so the temperature rise will not cause obvious performance change of particles. Under a magnetic field, the soft magnetic particles are arranged into chains, and a magnetic force between particles is generated. This force is related only to the magnetic field strength and is the component in the shear direction since there is a shear angle between particle chain and magnetic field. The sum of the magnetic force between particles is the shear stress when the particle chains are broken, which is shear yield stress. Therefore,

$$\tau_m = \tau_0 \quad (5)$$

(b) Force in base carrier fluid τ_η

Different from the particles, the base carrier fluid is more sensitive to temperature. The viscosity of base carrier fluid was obtained at different temperatures, as shown in Figure 8.

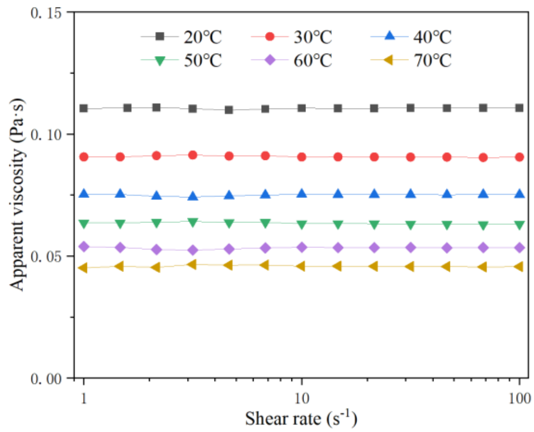

Figure 8 Viscosities of base carrier fluid at different temperatures

The viscosity of the base carrier fluid was almost constant at different shear rates, indicating that the base carrier fluid is a Newtonian fluid, so its average value was investigated. The viscosity of the base carrier fluid decreased significantly in response to the increase in temperature, but the decreasing trend became slower at high temperatures. The viscosity of the base carrier fluid decreased by 42.6% when the temperature was increased from 20 °C to 50 °C and by another 15.9% when the temperature was increased to 70 °C. The Andrade's formula (Andrade and Sciences 1940) is used to describe the temperature effects on the viscosity of the base carrier fluid at the temperatures below its boiling point, as shown in Equation (6).

$$\eta(T) = De^{\frac{E}{kT}} \quad (6)$$

where D is the test constant that can be obtained experimentally at different temperatures, k is the gas constant, T is the absolute temperature, E is the activation energy in viscous flow. Although the gas constant k and activation energy E would not be available, the parameters in Equation (6) can still be obtained from the two viscosities at the corresponding temperatures. When $B=E/k$, the Equation (6) can be expressed as

$$\eta(T) = De^{B/T} \quad (7)$$

where B and D can be obtained from Equations (8) and (9):

$$B = \frac{T_1 T_2 \ln(\eta_1 / \eta_2)}{T_2 - T_1} \ (8)$$

$$D = \frac{\eta_1}{e^{(B/T_1)}} \ (9)$$

where η_1 and η_2 are the viscosities of the base carrier fluid at the temperatures T_1 and T_2, respectively. As a consequence, the internal friction between base carrier fluid molecules can be obtained from Equation (10):

$$\tau_\eta = \eta(T)\dot{\gamma} \ (10)$$

In combination with Equation (10), the shear stress loss in the base carrier fluid can be obtained when the temperature rises from 20 ℃ to 70 ℃, as shown in Figure 9.

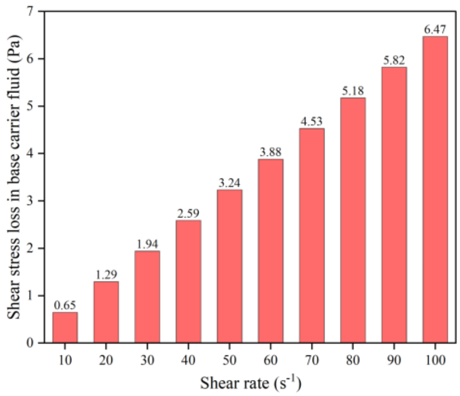

Figure 9 Shear stress loss in base carrier fluid in the temperature range between 20 ℃ and 70 ℃

The shear stress loss in the base carrier fluid increased linearly with shear rate, and the higher shear rate will cause higher shear stress loss. However, by comparing with Figure 5, the shear stress loss in the base carrier fluid decrease so little that it alone cannot explain the decrease in the shear stress of MR fluid. Besides, the internal friction in the base carrier fluid accounts only for a small percentage of the shear stress in the MR fluid, which was always less than 0.05% at different magnetic fields. As a consequence, the decrease in shear stress by temperature rise is not only due to the reduction of internal friction in the base carrier fluid, and the reduction in the friction force between the particles and base carrier fluid accounts for the main part of the decreases.

(c) Frictions between particle and based carrier fluid τ_h

Considering the discussion above, the force between particles and base carrier fluid is the key to investigate the decrease in shear stress with increasing temperature.

Previous studies have confirmed that the magnetic stress is influenced by several factors, such as particle size (Sarkar and Hirani 2015), particle shape (Bae et al. 2018), and particle permeability (Anupama et al. 2018, Kim et al. 2017). The following assumptions are made to simplify the analysis:

a) All particles are made of the same material and are spheres of the same size.

b) The magnetized particles are arranged in chains under magnetic field. The particle chains attach the upper and lower discs by the two ends.

c) The friction between the particle chains and the shear disc is strong enough so that there is no wall slip.

The continuous particle chains fracture into shorter chains under the action of shear. The short chains attached to the upper shear plane rotate with the upper shear disc where their velocity is the same with the upper shear disc because there is no wall slip. The rest of the particles attached to the lower shear plane remain stationary with the lower shear disc. The particle chains are continuously broken and reorganized in steady shear, as shown in Figure 10.

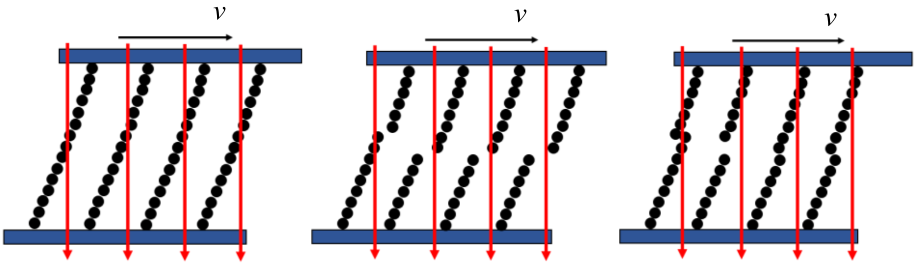

Figure 10 Evolution of particle chains in steady shear: (a) shear (b) break (c) recombination

The force between particles and base carrier fluid comes from the friction because there is a velocity difference between the particles and the carrier fluid when the particle chains attached to the rotating upper disk. There is also Brownian force, but it can be ignored since the mass fraction of particles is more than 20wt% (Sherman and Wereley 2013). In the absence of a magnetic field, the particles rotate at the same rate as the base carrier fluid under the action of internal friction. However, when a magnetic field is applied, the broken particle chains rotate at the same rate as the upper shear disc, while the base carrier fluid still rotates at the original rate, which results in a velocity difference between particles and base carrier fluid. This velocity difference causes the particles to be subjected to a hydrodynamic force during rotation, as shown in Figure 12. The hydrodynamic force is related to the shear rate, particle size, and the viscosity of base carrier fluid, following the Navier-Stokes Equation, as shown in Equation (11):

$$\tau_{N-S} = 6\pi\eta(T)vR \quad (11)$$

where v is the velocity difference between particles and base carrier fluid, and *R* is the particle radius.

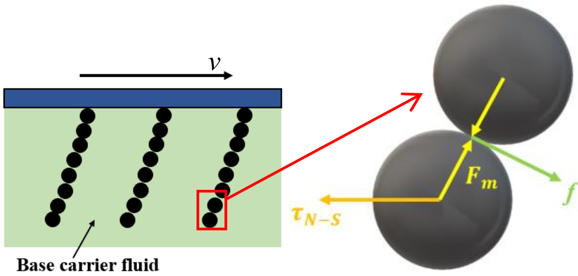

Figure 11 Force analysis of short particle chains during rotation

During rotation, the hydrodynamic force of an MR fluid is the sum of the hydrodynamic forces of all the rotating particles *N*, thus

$$\tau_h = N\tau_{N-S} \ (12)$$

5.2 Temperature effect under different magnetic field strengths

As stated in Section 4.2, the shear stress loss caused by temperature rise increases as the magnetic field strength increases. The shape of the particle chains changes with the shear rate, which results in the change of the number of particles rotating with the upper shear disc, and finally leads to different shear stresses. As magnetic field strength increases, more particles rotate with the upper shear disc. When the viscosity of the base carrier fluid decreases from the temperature rise, the losses caused by the hydrodynamic forces become more obvious with viscosity of base carrier fluid decreasing from temperature rise, as can be concluded from Equations (11) and (12).

However, the influence degree on the shear stress reduces when the temperature rises, which can be explained by the Mason number *Mn* that is the ratio of viscous resistance to magnetic force (Susan-Resiga and Vekas 2017):

$$Mn = \frac{\tau_h}{\tau_m} \quad (13)$$

At room temperature, the Masson number Mn is considered to be positively correlated with the magnetic field shear rate and negatively correlated with the magnetic field, as Equation (14) shows

$$Mn \propto \frac{\dot{\gamma}}{H^2} \quad (14)$$

where H is the magnetic field strength. However, with the increase in the temperature, the Masson number is also a function of temperature, since the viscosity of base carrier fluid changes with temperature. As a consequence, the temperature-dependent Masson number $Mn(T)$ is expressed as

$$Mn(T) \propto \frac{\dot{\gamma}\eta(T)}{H^2} \quad (15)$$

As a consequence, the ratio of hydrodynamic force to shear stress is

$$\frac{\tau_h}{\tau} = \frac{\tau_h}{\tau_y + \tau_h} = \frac{1}{\frac{1}{Mn} + 1} \quad (16)$$

In combination with Equations (15) and (16), it can be seen that the Mason number decreases rapidly with the increase in magnetic field strength, which is also the ratio of hydrodynamic force to shear stress decreases. Therefore, as the magnetic field strength increases, the decrease in hydrodynamic force caused by temperature rise has a less effect on the shear stress.

5.3 Accuracy of temperature-dependent model

In order to verify the accuracy of the novel constitutive model, the shear stresses of MRF 132DG at different temperatures were obtained at 325 mT, as shown in Figure 12. Figure 12 also compares the model constitutive model and the Herschel-Bulkley model obtained at room temperature.

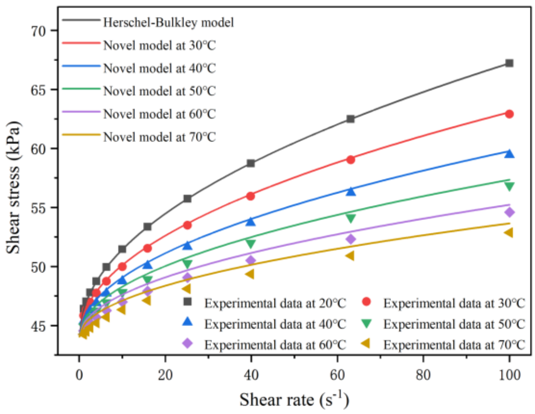

Figure 12 Accuracy analysis of novel constitutive model at different temperatures

As the shear stress also changes with magnetic field strength, the novel temperature-dependent model was also verified at different magnetic fields, as shown in Figure 13. In Figure 13, the point is the experimental data while the line is constitutive model.

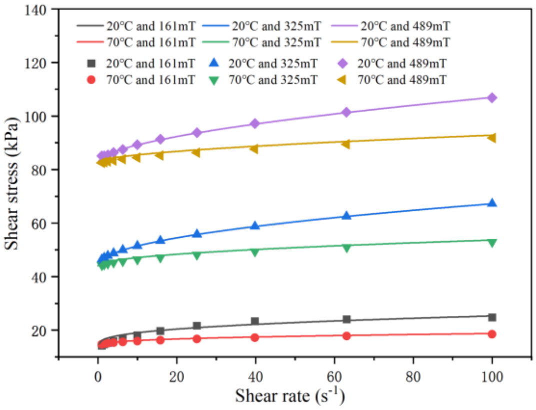

Figure 13 Accuracy analysis of novel constitutive model under different magnetic field strengths

As the Figure 12 shows, the temperature-dependent model can well describe the properties of MR fluids at different temperatures. The maximum relative errors of the temperature-dependent model are 1.1% at 50 ℃ and 1.9% at 70 ℃, while the relative errors of Herschel-Bulkley model are 18.2% and 27.1% under the same condition. Compared with the Herschel-Bulkley model, the temperature-dependent model has a 90% decrease in relative error, showing an excellent accuracy. As shown in Figure 13, the novel temperature-dependent model also has an excellent accuracy at different magnetic field strengths, of which the maximum relative error is 2.0%, 1.9% and 1.4% at 161 mT, 325 mT and 489 mT, respectively.

As can be seen from Figures 12 and 13, the shear stress obtained from the novel temperature-dependence model is always higher than the experimental data. In the novel temperature-dependent model, the force between soft magnetic particles is expressed as the shear yield stress at room temperature, but the temperature rise will result in a decrease in saturation magnetization, leading to a lower shear yield stress. Even if the temperature increase of 50 °C only reduces the shear yield stress by 1.8%, it will have an adverse effect on the accuracy of the model. Besides, this error might also result from the inevitable wall slip especially at higher shear rates.

Based on another MR fluid (Chen, et al. 2020), the experiments in this section were repeated to verify the accuracy of the novel temperature-dependent model for different MR fluid. For this MR fluid, the maximum relative errors of the novel temperature-dependent model are 2.1% and 1.7% at different temperatures and magnetic field strengths, respectively. The results show that the novel temperature-dependent model can well describe the properties of different MR fluids. Therefore, the temperature-dependent constitutive model has an excellent accuracy, which allows the properties of an MR fluid to be widely characterized only in a few experiments.

6. Conclusions

This paper investigates the influence of temperature rise on the properties of MR fluids. It is found that the zero-field viscosity of the MR fluids decreases with increasing temperature, and this phenomenon is more obvious at higher shear rates. Under a magnetic field, the shear stress of MR fluids also decreases significantly with an increasing temperature, and further decrease appears at higher shear rates. As the magnetic field strength increases, the temperature rise will cause a higher shear stress loss of MR fluid, but its relative influence decreases gradually. The Herschel-Bulkley model with high accuracy at room temperature is no longer able to accurately describe the shear stress of MR fluids at high temperatures. Its error is even up to 21.4% at 70 °C and will continue to increase as temperature rises.

The components of shear stress in MR fluids are analyzed to investigate the mechanism of temperature effect on shear stress of MR fluid. It is found that the force between particles barely changes and the change of force in base carrier fluid is so small that it can be ignored. The decrease in shear stress caused by temperature rises is mainly due to the change in hydrodynamic force between particles and base carrier fluid. The hydrodynamic force follows the Navier-Stokes law where the temperature-dependent viscosity of base carrier fluid follows the Andrade's formula. On this basis, a novel constitutive model with temperature prediction is proposed and the experimental results show that the error of the novel constitutive model decrease by 90% at different temperatures and magnetic field strengths, exhibiting an excellent accuracy. This temperature-dependent constitutive model allows the properties of an MR fluid to be widely characterized only in a few experiments.

Acknowledgements

This research is supported by joint Ph.D. program of 'double first rate' construction disciplines of CUMT.

References

Andrade E (1940), The viscosity of liquid. Proceedings of the Physical Society 52(6): 748.

Anupama AV, Kumaran V, Sahoo B (2018) Steady-shear magnetorheological response of fluids containing solution-combustion-synthesized Ni-Zn ferrite powder. Adv Powder Technol 29(9): 2188-2193. DOI 10.1016/j.apt.2018.06.002

Arora K, Singh AK (2020) Magnetorheological finishing of UHMWPE acetabular cup surface and its performance analysis. Mater Manuf Process 35(14): 1631-1649. DOI 10.1080/10426914.2020.1784928

Bae DH, Han WJ, Gao CY, Dong YZ, Choi HJ (2018) Preparation and Magnetorheological Response of Triangular-Shaped Single-Crystalline Magnetite Particle-Based Magnetic Fluid. IEEE T Magn 54(11):. DOI 10.1109/tmag.2018.2832166

Bahiuddin I, Mazlan SA, Shapiai I, Imaduddin F, Ubaidillah, Choi S-B (2018) Constitutive models of magnetorheological fluids having temperature-dependent prediction parameter. Smart Mater Struct 27(9):. DOI 10.1088/1361-665X/aac237

Chen F, Li H, Han M, Tian Z, Li A (2020) Preparation of magnetorheological fluid with excellent sedimentation stability. Mater Manuf Process 35(20): 1077-1083. DOI 10.1080/10426914.2020.1765250

Chen S, Huang J, Jian K, Ding J (2015) Analysis of Influence of Temperature on Magnetorheological Fluid and Transmission Performance. Adv Mater Sci Eng ():. DOI 10.1155/2015/583076

Chen S, Yang J (2019) Probing Slip Differential Heat of Magnetorheological Fluids Subjected to Shear Mode Operation and Its Effect on the Structure. Materials 12(11):. DOI 10.3390/ma12111860

Choi YT, Bitman L, Wereley NM (2005) Nondimensional analysis of electrorheological dampers using an eyring constitutive relationship. J Intel Mat Syst Str 16(5): 383-394. DOI 10.1177/1045389x05050529

Cvek M, Mrlik M, Pavlinek V (2016) A rheological evaluation of steady shear magnetorheological flow behavior using three-parameter viscoplastic models. J Rheol 60(4): 687-694. DOI 10.1122/1.4954249

Desai RM, Acharya S, Jamadar M-e-H, Kumar H, Joladarashi S, Sekaran scR (2020) Synthesis of magnetorheological fluid and its application in a twin-tube valve mode automotive damper. P I Mech Eng L-J Mat 234(7): 1001-1016. DOI 10.1177/1464420720925497

Jonkkari I, Kostamo E, Kostamo J, Syrjala S, Pietola M (2012) Effect of the plate surface characteristics and gap height on yield stresses of a magnetorheological fluid. Smart Mater Struct 21(7): . DOI 10.1088/0964-1726/21/7/075030

Kikuchi T, Abe I, Nagata T, Yamaguchi A, Takano T (2020) Twin-driven actuator with multi-layered disc magnetorheological fluid clutches for haptics. J Intel Mat Syst Str 32: 1313-1322. DOI 10.1177/1045389x20943958

Kim MH, Choi K, Nam JD, Choi HJ (2017) Enhanced magnetorheological response of magnetic chromium dioxide nanoparticle added carbonyl iron suspension. Smart Mater Struct 26(9):. DOI 10.1088/1361-665X/aa7cb9

Kubik M, Pavlicek D, Machacek O, Strecker Z, Roupec J (2019) A magnetorheological fluid shaft seal with low friction torque. Smart Mater Struct 28(4):. DOI 10.1088/1361-665X/ab0834

Lv H, Chen R, Zhang S (2018) Comparative experimental study on constitutive mechanical models of magnetorheological fluids. Smart Mater Struct 27(11):. DOI 10.1088/1361-665X/aae5e6

Malik MY, Khan M, Salahuddin T, Khan IJES, Journal TaI (2016) Variable viscosity and MHD flow in Casson fluid with Cattaneo–Christov heat flux model: Using Keller box method. Eng Sci Technol 19(4): 1985-1992

Maroofi J, Hashemabadi SH (2019) Experimental and numerical investigation of parameters influencing anisotropic thermal conductivity of magnetorheological fluids. Heat and Mass Transfer 55(10): 2751-2767. DOI 10.1007/s00231-019-02618-w

Papanastasiou TC (1989) Flows of Materials with Yield. J Rheol 31(5): 385-404

Pelegrine DH, Silva FC, Gasparetto CA (2002) Rheological behavior of pineapple and mango pulps. Lebensm-Wiss Technol 35(8): 645-648. DOI 10.1006/fstl.2002.0920

Rabbani Y, Ashtiani M, Hashemabadi SH (2015) An experimental study on the effects of temperature and magnetic field strength on the magnetorheological fluid stability and MR effect. Soft Matt 11(22): 4453-4460. DOI 10.1039/c5sm00625b

Rosensweig, Ronald E (1995) On magnetorheology and electrorheology as states of unsymmetric stress. J Rheol 39(1): 163-188

Saha P, Mukherjee S, Mandal K (2019) Rheological response of magnetic fluid containing Fe3O4 nano structures. J Magn Magn Mater 484: 324-328. DOI 10.1016/j.jmmm.2019.04.055

Sahin H, Wang X, Gordaninejad F (2009) Temperature Dependence of Magneto-rheological Materials. J Intel Mat Syst Str 20(18): 2215-2222. DOI 10.1177/1045389x09351608

Sarkar C, Hirani H (2015) Effect of Particle Size on Shear Stress of Magnetorheological Fluids. Smart Sci 3(2): 65-73.

Sherman SG, Wereley NM (2013) Effect of Particle Size Distribution on Chain Structures in Magnetorheological Fluids. IEEE T Magn 49(7): 3430-3433. DOI 10.1109/tmag.2013.2245409

Susan-Resiga D, Vekas L (2017) Ferrofluid based composite fluids: Magnetorheological properties correlated by Mason and Casson numbers. J Rheol 61(3): 401-408. DOI 10.1122/1.4977713

Tian Z, Wu X, Xiao X, Chen F (2019) A Novel Preparation Process for Magnetorheological Fluid with High Working Temperature. Journal of Magnetics 24(4): 634-640. DOI 10.4283/jmag.2019.24.4.634

Wang D, Zi B, Zeng Y, Hou Y, Meng Q (2014) Temperature-dependent material properties of the components of magnetorheological fluids. J Mater Sci 49(24): 8459-8470. DOI 10.1007/s10853-014-8556-x

Williams EW, Rigby SG, Sproston JL, Stanway RJJJoN-NFM (1993) Electrorheological fluids applied

to an automotive engine mount. J Non-Newton Fluid 47: 221-238
Wu X, Xiao X, Tian Z, Chen F, Jian W (2016) Effect of Particle Characteristics and Temperature on Shear Yield Stress of Magnetorheological Fluid. J Magn 21(2): 244-248. DOI 10.4283/jmag.2016.21.2.244
Yildirim G, Genc S (2013) Experimental study on heat transfer of the magnetorheological fluids. Smart Mater Struct 22(8): . DOI 10.1088/0964-1726/22/8/085001
Yoon D-S, Kim G-W, Choi S-B (2021) Response time of magnetorheological dampers to current inputs in a semi-active suspension system: Modeling, control and sensitivity analysis. Mech Syst Signal Pr 146(): . DOI 10.1016/j.ymssp.2020.106999